Comparative optical study of the two-dimensional donor-type intercalation compounds graphite-KH_x and their binary counterparts C_8K and $C_{24}K$

G. L. Doll, M. H. Yang, and P. C. Eklund
Department of Physics and Astronomy, University of Kentucky, Lexington, Kentucky 40506
(Received 27 May 1986; revised manuscript received 17 February 1987)

We report the results of optical reflectivity studies of the stage-1 and -2 graphite-KH_x intercalation compounds prepared by direct reaction of highly ordered pyrolytic graphite and KH powder. The stage-1 and -2 binary graphite-K compounds are studied for comparison. The optical data are analyzed in terms of a model involving two-dimensional (2D) graphitic π electrons and three-dimensional (3D) nearly free K($4s$) electrons. The model is used to interpret the observed values of the free-carrier unscreened plasma frequencies and the position of the interband absorption threshold to determine experimental values for the Fermi level (E_F) in the carbon π band(s) and the fractional occupation of the K($4s$) band. For the hydrides, we find quantitative evidence that the hydrogen states lie below E_F. Thus, hydrogen is present as H^-, acting as an acceptor, thereby compensating the electron donation to the π bands from the K($4s$) states. This assumption and the optical data for the stage-1 and -2 hydrides results in a [H]/[K] ratio of 0.8, in excellent agreement with chemical analyses reported by Guérard and co-workers, and leads to very small values for the fractional K($4s$) band occupation $f_K < 0.03$ electrons per K atom. Within the framework of a superimposed 2D (π) and 3D [K($4s$)] rigid-band model, our experimental results support an empty K($4s$) band (i.e., $f_K = 0$) in stage-2 $C_{24}K$. In stage-1 C_8K, the rigid-band model yields large values for f_K ($f_K > 0.5$ electrons per K atom), unless the value of the optical mass of the electrons in the K($4s$) states is larger than ~ 2. The C_8K results are also discussed in terms of more sophisticated energy-band calculations.

I. INTRODUCTION

It has been known for some time that gaseous hydrogen can be chemisorbed into the binary graphite intercalation compound (GIC) C_8K to form the ternary GIC hydride $C_8KH_{2/3}$.[1-3] The reaction rate is prohibitively slow in well-ordered graphite, even at several atmospheres of hydrogen pressures,[4] and is therefore carried out on C_8K powder. The binary GIC is a stage-1 compound, whereas the ternary hydride GIC is a stage-2 compound—the stage index refers to the number of carbon layers stacked between successive intercalate layers.[5,6] It has also been reported[4] that a larger [H]/[K] ratio of 0.8 can be accomplished by reacting pyrolytic graphite directly with KH powder to form either a stage-1 ($C_4KH_{0.8}$) or a stage-2 ($C_8KH_{0.8}$) compound, depending on the reaction temperature. We report here on the results of optical reflectivity studies of these hydride GIC's prepared from KH powder and highly oriented pyrolytic graphite which we refer to as graphite-KH_x. Optical data of the binary graphite-K compounds C_8K and $C_{24}K$ are presented and analyzed for comparison with the graphite-KH_x compounds. The optical data indicate that the electron transfer from the K($4s$) band to the lower-lying graphitic π^* and H($1s$) levels (bands) is complete, or nearly so. The large thickness of the trilayer intercalate sandwich (K-H-K) serves to decouple the C-C interactions along the c axis resulting in a quasi-two-dimensional (2D) donor-type GIC, with a basal-plane conductivity associated with the π^* conduction band. The term donor type refers to the fact that the insertion of the intercalate layers raises the electron concentration in the carbon π conduction bands(s) due to a donation of electrons from the intercalate to the carbon layers.[5,6]

The trilayer intercalate sandwich structure of graphite-KH_x (K-H-K) is similar to that reported[7] for graphite-KHg (K-Hg-K). Using transmission electron microscopy (TEM) both of these ternary GIC's have been found[8,9] to exhibit both the $(2\times 2)R0°$ and $(\sqrt{3}\times\sqrt{3})R30°$ in-plane intercalate-layer superlattice phases. In the case of graphite KH_x, the TEM patterns are sensitive only to the position of the C and K atoms. On the basis of ($hk0$) diffraction studies, Guérard *et al.*[4] have identified the presence of a $2\sqrt{3}\times 3$ rectangular ordering of the intercalate layer. Recent studies involving in-plane elastic neutron scattering measurements by Kamitakahara *et al.*[10] are consistent with the observations of Guérard *et al.* The neutron scattering results[10] on the hydride GIC's indicate that the H atoms themselves form an ordered sublattice, rather than randomly decorating the K superlattice. ac magnetic-susceptibility measurements[11] found $C_8KH_{0.8}$ (stage 2) to be superconducting, but $C_4KH_{0.8}$ (stage 1) was not found to superconduct for $T > 70$ mK at ~ 1 atm. Resistivity studies[12] found a linear T dependence for $4.2 < T < 300K$ for both stage-1 and -2 graphite KH_x. This behavior is not observed in the binary donor-type GIC's, but has also been reported[12] in the stage-1 and -2 graphite-KHg compounds—which also superconduct[11] ($T_c = 0.77$ K for C_4 KHg, $T_c = 1.90$ K for C_8KH_g). Further recent measurements on graphite KH_x which are relevant to the study presented here are magnetic susceptibility[13] and Raman scattering.[14] References to recent re-

sults on the related stage-2 hydride—$C_8KH_{2/3}$, prepared by the reaction of powdered C_8K with gaseous hydrogen, can be found in Ref. 15.

II. EXPERIMENTAL DETAILS

The graphite-KH_x compounds were obtained by immersing plates ($7\times7\times0.3$ mm^3) of highly oriented pyrolytic graphite (HOPG, Union Carbide) in KH powder (Morton Thiokol/Alpha Inc.) at elevated temperature. The stage-1 and -2 compounds resulted, respectively, from reactions carried out for 7 days at $T=350$ °C and $T=250$ °C. The KH powder, as received, was light gray in color and immersed in mineral oil. To separate the KH from the oil, the mixture was loaded into a glass vacuum apparatus above a clean sintered glass filter disk (Ace) with pore diameters in the range 70—100 μm. The space above and below the filter disc was evacuated for ~1 h to a pressure of 10 μm using a liquid-nitrogen-trapped forepump. An overpressure of ultra high purity UHP grade N_2 (~2 atm) was then introduced above the KH-oil mixture to force the oil through the disk, leaving a residue of oil and the KH powder behind. Spectral-grade pentane was next admitted through a valve in a side arm above the disk to dissolve the oil residue. The solvated oil was then pushed through the disc by introducing UHP N_2 again. The remaining KH powder was then pumped for ~8 h to remove any remaining pentane. More details of the vacuum-line technique for separation of oil and air-sensitive powders are available in the literature.[16]

Following the method of Guérard *et al.*,[4] the HOPG and KH powder was sealed off in 2-mm-wall Pyrex tubing (10-mm inside diameter) under a diffusion-pump vacuum ($\sim10^{-6}$ Torr). Some concern must be given to the wall thickness of the reaction ampoules—the walls are weakened somewhat by attack from K and can burst due to a gas overpressure which presumably occurs upon dissociation of the KH at the reaction temperature. Also, it should be denoted that KH is pyrophoric and therefore *should not be handled in room air.* The color of the HOPG plates reacted at 350 °C (stage 1) and 250 °C (stage 2) was observed to be violet and blue, respectively. The samples were removed from the reaction ampoules in a high-quality He-atmosphere glove box (Vacuum Atmospheres, Inc., p_{H_2O} and $p_{O_2}<1$ ppm), cleaved and transferred to rectangular cross section uv-quartz ampoules ($0.4\times0.8\times8$cm^3) (Vitrodynamics) which were sealed under vacuum ($\sim10^{-6}$ Torr) for the optical measurements.

The samples were characterized in the deep bulk and in the optical skin depth (~1000 Å), respectively, by (00l) x-ray diffraction and Raman scattering probes. The Raman results will be discussed later in the paper. A General Electric XRD6 diffractometer equipped with a Si:Li detector and Mo source was used to collect the (00l) data which showed little or no evidence for stage impurity or inclusion of the K-based binary GiC's. We note that a pure stage-2 graphite-KH_x is more difficult to achieve—often times containing $C_{24}K$ as a minority phase. The c-axis separation of intercalate layers (I_c) was determined using Bragg's law and the method of least squares to be $I_c=8.53\pm0.02$ Å (stage 1) and $I_c=11.89\pm0.02$ Å (stage 2). These values agree, within experimental error, with the literature.[4] Our stage-1 I_c value corresponds to the value reported[4] for the alpha phase; the beta phase ($I_c=9.13$ Å) (Ref. 11) was not present in the samples studied in this work. We have, however, observed the beta and alpha hydride phases coexisting in some stage-1 samples. The stage-1 (alpha) and stage-2 hydride I_c values differ by 3.35 Å, which is the accepted value[5,6] for the thickness of a graphitic C layer. This suggests that the nature of the intercalate layers for these stage-1 and -2 compounds is similar, if not the same.

The Raman scattering measurements on the intercalant-perturbed graphitic intralayer phonons (~1600 cm^{-1}) were carried out in the Brewster angle backscattering geometry under low laser power (4880 Å at ~20 mW).[17] Reflectivity measurements (R) were carried out at near-normal incidence using a prism monochromator and a standard MgF_2-overcoated Al mirror calibrated against a Ag film below 3 eV and calibrated absolutely for $E>3$ eV. Spectra were obtained in the range of transmission of the quartz ampoule ($0.5<\hbar\omega<6$ eV). Details of the Raman and reflectance apparatus are available in the literature.[17,18] The absolute scale of the reflectance data was checked at $E=1.96$ eV using a He-Ne laser. To perform Kramers-Krönig (KK) analyses, the spectra were extended in the ir as a Drude metal, and in the uv as a density-scaled spectrum of pristine graphite. The KK transform of the reflectance (R) data (i.e., the phase integral) was then calculated to obtain the dielectric functions ϵ_1 and ϵ_2. Further details of the KK transformation and the data analysis are given in a recent review.[19]

III. RESULTS AND DISCUSSION

Raman scattering studies of the intercalant-perturbed graphitic phonon at ~1600 cm^{-1} provide an important stage-specific characterization[20] of the bulk in the optical skin depth (~1000 Å). In Fig. 1 we display the Raman spectra in the vicinity of the ~1600-cm^{-1} graphitic intralayer phonons for the same samples whose reflectance spectra are analyzed below. The solid lines in the lower three spectra are the result of least-squares fits to a single Lorentzian line shape. The C_8K spectrum appears in the inset in the figure because an otherwise narrow peak associated with the intralayer phonon is broadened and downshifted by a Breit-Wigner or Fano resonance characteristic of the stage-1 C_8K, C_8Rb, and C_8Cs compounds.[21,22] $C_{24}K$, $C_4KH_{0.8}$, and $C_8KH_{0.8}$ exhibit a Lorentzian rather than Breit-Wigner line shape, indicating that in these compounds the coupling between the graphitic phonons (E_{2g}, Γ point) and a Raman-active continuum is much weaker. The strong coupling which occurs in the stage-1 GIC's C_8K, C_8Rb, and C_8Cs downshifts the graphitic interlayer phonon structure from ~1600 to ~1500 cm^{-1}.[17,20,21] It is evident in Fig. 1 that the linewidth for the $C_{24}K$ binary GIC [full width at half maximum (FWHM) of 12 cm^{-1}] is noticeably less than the ternary hydrides (FWHM of ~23 cm^{-1}). This might be interpreted as evidence for a generally poorer in-plane order, or poor stacking fidelity in the ternaries. However,

linewidths for $C_{24}Cs$ and $C_{24}Rb$ have also been reported to be ~ 22 cm^{-1} (Ref. 20) and the linewidths for C_6Li (stage 1) and $C_{12}Li$ (stage 2) are found to be in excess of ~ 30 cm^{-1}.[23,24] The line-shape parameters for the spectra in Fig. 1 appear in Table I. The frequency values we observe for the stage-1 and -2 graphite-KH_x compounds are in reasonable agreement with the recent work of Yeh *et al.*[14]

In Fig. 2 we display the reflectance spectra $R(E)$ of C_8K, $C_{24}K$, $C_4KH_{0.8}$, and $C_8KH_{0.8}$. The spectra are characteristic of metals, exhibiting a sharp Drude edge in the visible region. The edge position, which is located near the *screened* plasma frequency $\tilde{\omega}_p$, is largely responsible for the characteristic color of the compounds. The rise in the reflectance with increasing energy from the minimum is associated with the threshold for interband absorption. The broad peak in the range 4—5 eV is the GIC analog of the M-point absorption[25] observed in pristine graphite.[26] The binary GIC spectra ($C_{24}K$, C_8K) are in good agreement with that observed previously.[27,28]

In Figs. 3 and 4 we display ϵ_2 data obtained by KK analyses (Sec. II). The stage-1 compounds C_8K and $C_4KH_{0.8}$, and the stage-2 compounds $C_{24}K$ and $C_8KH_{0.8}$ are compared in Figs. 3 and 4, respectively. The insets to the figures show the zero crossing of ϵ_1 which locates the *screened* plasma frequency $\tilde{\omega}_p$ and thus the position of the intraband plasmon observable in electron-energy-loss spectroscopy.[29–31] The downshift of $\tilde{\omega}_p$ we observe for the ternary hydride relative to the parent binary GIC indicates a decrease in the Fermi energy E_F in the carbon π band. This can be understood as result of the introduction of low-lying H($1s$)-states in the graphite-KH compounds.

Our schematic density of states (DOS) model for $C_4KH_{0.8}$ and $C_8KH_{0.8}$ is shown in Fig. 5. The position of the low-lying H states is consistent with the large electronegativity of hydrogen. Electrons must empty from the π conduction band and the K($4s$) band to fill these low-lying H($1s$) levels (band). Our data also support the placement of E_F *below* the K($4s$) band minimum. We discuss the evidence for an empty K($4s$) band in the hy-

TABLE I. Results of 00l x-ray diffraction (I_c), Raman scattering (ω,Γ) and optical reflectivity ($\omega_p,\omega_p\tau,\epsilon_\infty,E_T/2$) studies of C_8K, $C_4KH_{0.8}$, $C_{24}K$, $C_8KH_{0.8}$. The various parameters are defined in the text.

Nominal formula	Stage index	I_c (Å)	Raman line-shape parameters: Peak position (cm^{-1})	Raman line-shape parameters: FWHM (cm^{-1})	Drude Parameters[a]: $\hbar\omega_p$[b] (eV)	$\omega_p\tau$	ϵ_∞	f_C[b]	E_F[b] (eV)	$E_T/2$[a,b] (eV)
C_8K	1	5.35±0.02 5.35[c]	1522±2[d]		4.51±0.1 4.5[f] 4.65[d]	14	3.6	~1/8[d] ~0.6/8[g] ~0.6/8[h]	1.4[d] 1.4[g] 1.4[h]	1.60 1.50[f] 1.45[d] 1.45[g]
$C_4KH_{0.8}$	1	8.53±0.02 8.53[j] 8.56[m]	1596±2 1596±3[k]	25±2 23±3[k]	3.31±0.1	17	3.0	0.050±0.006[i] 0.054±0.005[l] 0.020[m]	1.53±0.09[i] 1.62±1[l] 0.65[m]	1.40
$C_{24}K$	2	8.74±0.02 8.74[e]	1601±2 1599[n]	13±2 13[n]	4.2±0.1	21	6.3	0.042±0.004[l] 0.042[o]	1.42±0.07[l]	1.40
$C_8KH_{0.8}$	2	11.89±0.02 11.88[j] 11.93[m] 12.08[k]	1598±2 1598±3[k]	26±2 12±3[k]	3.26±0.1	20	4.3	0.026±0.003 0.033[m]	1.13±0.7[l] 1.15[m]	1.10

[a]Obtained from fits of Eq. (1) to both R and ϵ_2 data.
[b]Purely theoretical values obtained from band-structure calculations are underlined.
[c]This feature exhibits a Breit-Wigner line shape, the remaining Raman data in the table refer to Lorentzian line shapes.
[d]DiVincenzo and Rabii (Ref. 37).
[e]Parry and Nixon (Ref. 40).
[f]Fischer *et al.* (Ref. 27).
[g]Ohno *et al.* (Ref. 36).
[h]Tanuma *et al.* (Ref. 42).
[i]Obtained from our value for ω_p and the band model of Holzwarth, Ref. 33.
[j]Guérard *et al.* (Ref. 4).
[k]Yeh *et al.* (Ref. 14).
[l]Obtained from our value for ω_p and the band model of Blinowski *et al.* ($\gamma_0=2.9$ eV, $\gamma_1=0.375$ eV), Ref. 32.
[m]Enoki *et al.* (Ref. 39).
[n]Dresselhaus and Dresselhaus (Ref. 20).
[o]Dresselhaus *et al.* (Ref. 41).

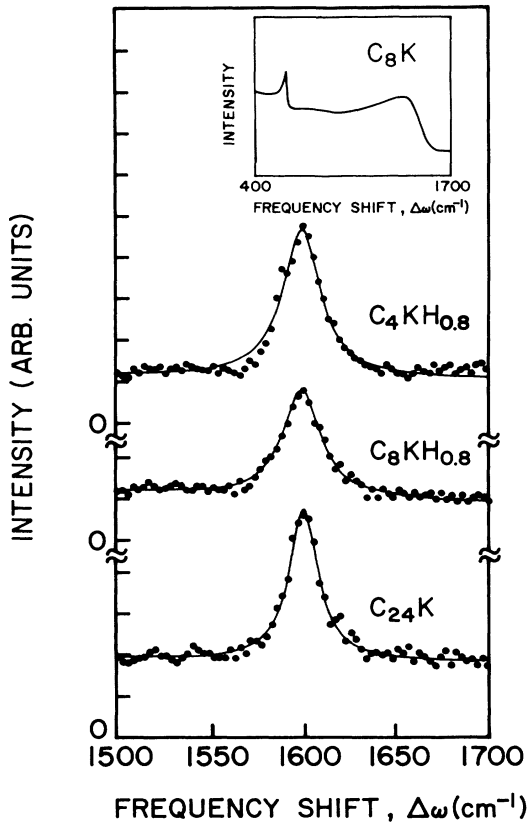

FIG. 1. Raman spectra associated with the high frequency (~ 1600 cm^{-1}) graphitic intralayer phonons for the stage-1 and -2 binary (C_8K, $C_{24}K$) and ternary ($C_4KH_{0.8}$), $C_8KH_{0.8}$) GIC's. The C_8K spectrum (inset) exhibits a Breit-Wigner line shape typical of the C_8M (M=K,Cs,Rb) compounds while $C_{24}K$, $C_4KH_{0.8}$, and $C_8KH_{0.8}$ spectra exhibit a Lorentzian line shape. Data are shown as points while the solid lines represent the results of least-square fits of the spectra to Lorentzian line shapes.

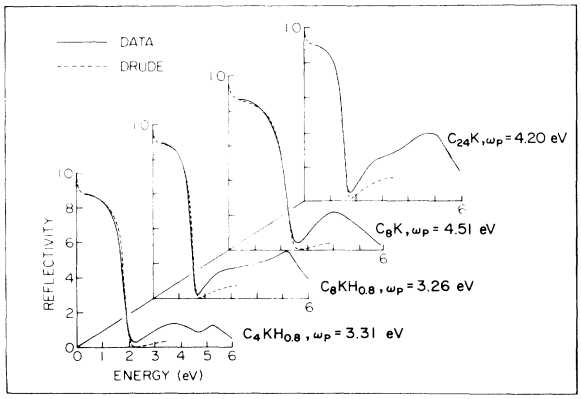

FIG. 2. Reflectance data (300 K) measured at near-normal incidence to the c face for C_8K, $C_{24}K$, $C_4KH_{0.8}$, and $C_8KH_{0.8}$. Data are displayed as solid lines while the dashed lines are calculated from Drude parameters obtained from Fig. 6. Values of the corresponding unscreened or bare plasma frequencies (ω_p) are displayed beside each spectrum.

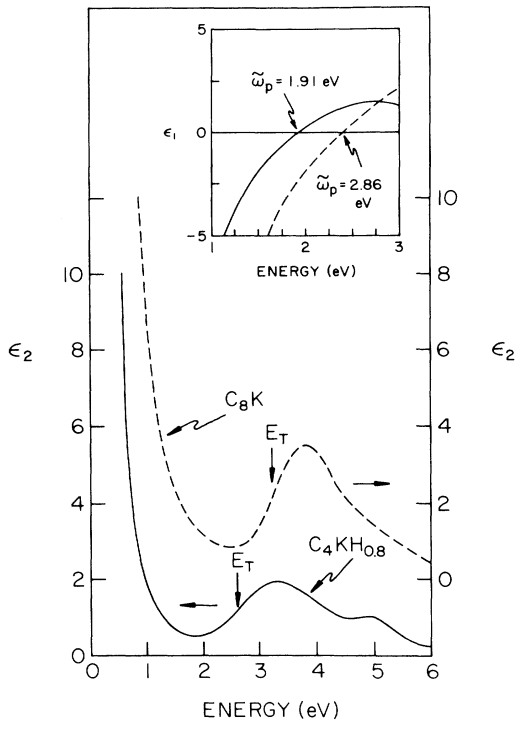

FIG. 3. Real (ϵ_1) and imaginary (ϵ_2) dielectric functions for $C_4KH_{0.8}$ (solid line) and C_8K (dashed line). The inset shows the zero crossing of ϵ_1 which approximately locates the screened plasma frequency ($\tilde{\omega}_p$). The arrows associated with energy E_T indicate the midpoint of the interband threshold. The threshold is broadened by electron-electron scattering (Ref. 38).

drides in detail below.

The contribution to the optical dielectric function $\epsilon(0,\omega)=\epsilon_1+i\epsilon_2$ from free carrier (or intraband) absorption is given in the Drude approximation by the well-known expression

$$\epsilon_{\text{Drude}}=\epsilon_\infty-\omega_p^2(\omega^2+i\omega/\tau)^{-1}\ , \tag{1}$$

where ω_p is the *unscreened* plasma frequency, τ is the average carrier lifetime, and ϵ_∞ if the core dielectric constant. If there is more than one partially occupied band, then the standard approximation is to assume $\tau_j\cong\tau_0$, independent of band index j. Then the plasma frequency in Eq. (1) is given by

$$\omega_p^2=\sum_j \omega_{p,j}^2\ , \tag{2}$$

where

$$\omega_{p,j}^2=4\pi N_j e^2/m_{\text{opt},j}\ . \tag{3}$$

N_j is the carrier concentration, $m_{\text{opt},j}$ is the optical mass, and e is the electronic charge. The alternative to this procedure is to assign different τ_j and adjust all $\omega_{p,j}$ and τ_j parameters to fit the data. This proliferation in the number of parameters is seldom justified, and we do not pursue it here.

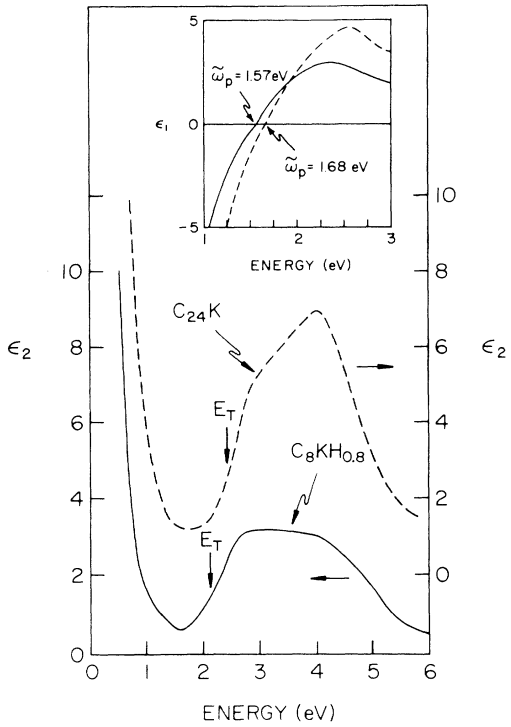

FIG. 4. Real (ϵ_1) and imaginary (ϵ_2) dielectric functions for $C_8KH_{0.8}$ (solid line) and $C_{24}K$ (dashed line). See caption to Fig. 3.

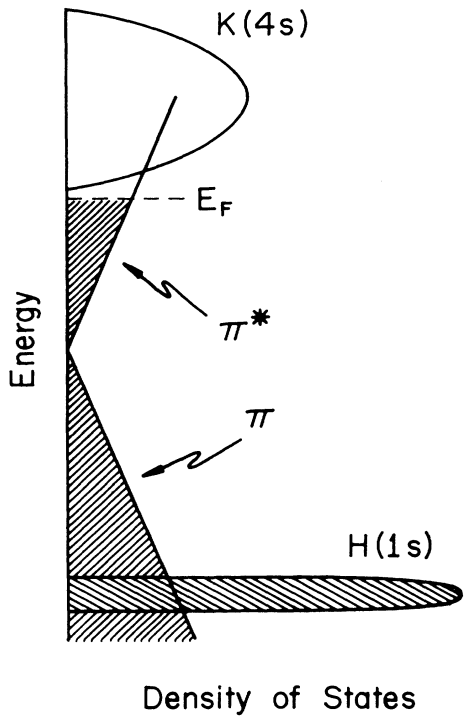

FIG. 5. Schematic density of states for $C_4KH_{0.8}$ and $C_8KH_{0.8}$. The H(1s) levels lie below the Fermi level E_F (dashed line) indicating the hydrogen is present as H^-.

In Fig. 2 the dashed lines indicate the reflectance calculated from Eq. (1) using a single ω_p and τ, and are in good agreement with the low-energy data below the reflectance minimum. The disagreement near, and just above, the minimum occurs because the presence of nearby interband absorption is inadequately described by a core dielectric constant ϵ_∞. In Fig. 6 we examine the Drude fit in a different way. We plot $(\omega\epsilon_2)^{-1}$ versus ω^2. This analysis yields a linear plot for a Drude metal [Eq. (1)], whose slope and intercept depend on the unscreened or "bare" plasma frequency ω_p and τ only, and not on ϵ_∞. The linear behavior at low energies is evident, the deviation from linearity at higher energy is due to the onset of interband absorption. The parameters obtained from the Drude analyses of R and ϵ_2 are found in Table I.

Referring to the schematic DOS diagram of Fig. 5, it is evident that charge neutrality and a stoichiometry $C_{4n}KH_x$ (where $n=1,2$ is the stage index) (Ref. 4) yield the following relationship relationship among the fractional band occupations f_X

$$(f_K-1)+x(f_H-1)+4nf_C=0\ , \tag{4}$$

where f_X (X=K,H,C) represents the number of electrons per X atom in the respective K(4s), H(1s), and $C(\pi^*)$

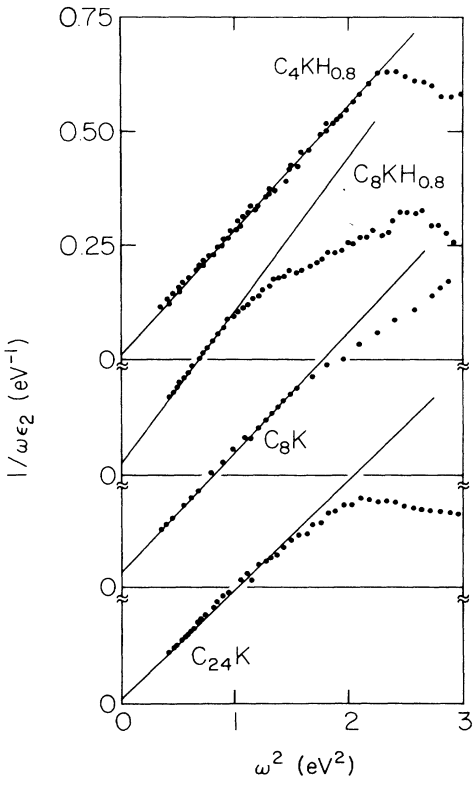

FIG. 6. Plot of $(\omega\epsilon_2)^{-1}$ vs $(\hbar\omega)^2$ for C_8K, $C_{24}KH_{0.8}$, and $C_8KH_{0.8}$. A linear curve indicates Drude behavior [Eq. (1)]. The corresponding values of the Drude parameters ω_p and $\omega_p\tau$ are given in Table I and are independent of the choice for the core dielectric constant ϵ_∞ used to calculate R (dashed curve in Fig. 2).

bands(s). The reaction of KH with graphite has been reported to lead to a [H]/[K] ratio $x=0.8$ for both the stage-1 and -2 hydrides.[4] If we adopt this value of x for the moment, and assume that the H levels (or band) lie below the Fermi level (i.e., $f_H=2$), then Eq. (4) can be written as

$$f_C=(0.2-f_K)/4n \ . \tag{5}$$

We can describe the stage-1 two-dimensional (2D) π^* conduction-band either by the tight-binding band model of Blinowski *et al.*[32] or the linear combination of atomic orbitals model of Holzwarth.[33] Previous work[34] has shown that both these models yields approximately the same values for $m_{\rm opt}$ for stage-1 GIC's, provided a value of the C-C intralayer interaction $\gamma_0 \sim 2.9$ eV is used in the model of Blinowski *et al.*[32] The bare plasma frequency for the stage-1 GIC is given in the Blinowski model by

$$\omega_p^2=4e^2E_F/\hbar^2 I_c \quad \text{(stage 1)} \ , \tag{6}$$

where E_F is given by

$$E_F=\gamma_0(\sqrt{3}\pi f_C)^{1/2} \quad \text{(stage 1 and 2)} \ . \tag{7}$$

Using Eqs. (2), (3) and (5)—(7) we express the bare plasma frequency as a sum of contributions from the π^* and K(4s) bands in terms of the fractional occupation of the K(4s) band f_K. The first and second terms on the right-hand side in Eq. (8) are, respectively, from the π and K(4s) bands,

$$\hbar^2\omega_p^2(\text{eV}^2)=7.87\gamma_0(0.2-f_K)^{1/2} + 15.4 f_K/m_K \quad (C_4KH_{0.8}) \ , \tag{8}$$

where $m_K=m_{\text{opt},K}/m_e$, and m_e is the electronic mass. We note that if $f_K=0$, the $K(4s)$ band is empty, and if $f_K=0.2$ the π band is empty (assuming [H]/[K]=0.8). In the left-hand panel of Fig. 7 we plot on an expanded vertical scale the square of the calculated plasma frequency versus f_K [Eq. (8)] for two choices of m_K and γ_0. ω_p^2 decreases for increasing f_K because the optical mass of the π electrons is considerably less than the free-electron mass values $m_K=1$—2 chosen for the K(4s) electrons. The values of γ_0 used are consistent with Holzwarth[33] and those used previously to describe optical results in graphite-$SbCl_5$ (Ref. 18) and graphite-H_2SO_4 (Ref. 34). However, St. Jean *et al.*[35] report somewhat lower values of γ_0 (2.6 eV for stage 1 and 2.8 eV for stage 2) on the basis of similar reflectance studies of graphite-H_2SO_4. As is evident from the left-hand panel of Fig. 7, values for $\gamma_0<2.9$ eV strengthen the argument that the K(4s) band is empty in $C_4KH_{0.8}$. The upper and lower arrows on the ordinate indicate, respectively, our experimental values for the most probable value of ω_p^2 and the lower bound for ω_p^2, consistent with an experimental uncertainty in the plasma frequency of ± 0.1 eV. The most probable experimental value for ω_p^2 lies above the uppermost calculated curve, indicating the K(4s) band is probably empty. However, our estimate for the lower bound on ω_p^2 cuts the upper curve at a very small value $f_K \sim 0.02$ electrons per K atom which represents the maximum occupation in the K(4s) band in the stage-1 hydride consistent with the in-

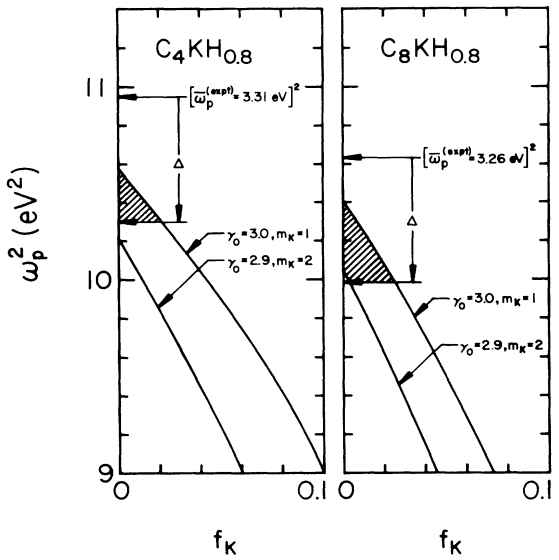

FIG. 7. Square of the plasma frequency (ω_p^2) vs f_K, where f_K is the fractional occupation of the K(4s) band. The left-hand panel is for stage-1 $C_4KH_{0.8}$ and the right-hand panel is for $C_8KH_{0.8}$. The curves are calculated according to the model described in the text for the values of the parameters (γ_0, m_K) shown. $\omega_p^{\rm expt}$ indicates the most probable value of the experimental plasma frequency. ω_p^2 is uncertain to $\pm\Delta$. $\omega_p^2-\Delta$ cuts the calculated curves as shown and leads to the corresponding estimate for the upper bound of f_K for the stage-1 and -2 hydrides.

traband optical data and $\Delta\omega_p=\pm 0.1$ eV. This small value of f_K coupled with a large value of I_c indicate that $C_4KH_{0.8}$ should exhibit a high electrical anisotropy, more in line with a typical stage-1 acceptor GIC rather than a typical stage-1 binary donor GIC.

Our stage-1 value for $\omega_p(C_4KH_x)=3.31$ eV may be interpreted from another perspective. We assume the K(4s) band is empty and calculate the value $x=$[H]/[K] consistent with a 2D analysis for the π^* band [Eqs. (6) and (7) and $\gamma_0=2.9$ eV) and H levels which lie below E_F. We then find that $x=0.79\pm 0.02$ using the model of Blinowski *et al.*[32] Using the results of Holzwarth[33] we find $x=0.80\pm 0.02$. Both values of x are in excellent agreement with the reported experimental value ($x=0.8$) based on chemical analysis.[4] In Table I we list the value for E_F for $C_4KH_{0.8}$ obtained from the experimental bare plasma frequency and the models of Holzwarth ($E_F=1.53$ eV) and Blinowski ($E_F=1.62$ eV). The Blinowski model[32] result is higher due to the K point expansion used as an approximation to recover explicit formulas which relate E_F to f_C.

We next analyze the stage-2 plasma frequencies in the same way, using the stage-2 relationship for $\omega_p(E_F)$ (Ref. 32) and Eqs. (2)—(5) and (7), to develop a numerical relationship between ω_p and f_K the fractional K(4s) band occupation. For the case of the binary $C_{24}K$ compound, the experimental value of $\omega_p=4.20\pm 0.1$ eV results in $f_K=0$ (i.e., complete charge transfer) and $f_C=1/(23.7\pm 0.12)$, in excellent agreement with the expected average

stoichiometry for stage-2 graphite-K.[5,6] For the stage-2 hydride, the numerical relation ω_p^2 versus f_K is plotted in the right-hand panel of Fig. 7 for (1) the values of γ_0 and the K electron optical mass m_K shown, (2) $I_c = 8.53$ Å, and (3) $\gamma_1 = 0.375$ eV,[32,18] where γ_1 is the C-C *inter*layer interaction. As in the case of the stage-1 hydride, the most probable experimental value for $\omega_p^2 = (3.26\text{ eV})^2$ lies slightly above the curves. Our lower estimate for ω_p^2, consistent with an experimental uncertainty $\Delta\omega_p = \pm 0.1$ eV, cuts the upper curve $\gamma_0 = 3$ eV, $m_K = 1$. In this latter case we obtain $f_K \sim 0.03$ electrons per K atom for an upper bound for the fractional occupation of the K($4s$) band for the stage-2 hydride with stoichiometry $C_8KH_{0.8}$.

On the other hand, if we (1) assume the K($4s$) band is empty and the H($1s$) levels lie below E_F, (2) use the stage-2 band model of Blinowski *et al.*,[32] and (3) use our value for $\omega_p = 3.26 \pm 0.1$ eV, we find $x = [\text{H}]/[\text{K}] = 0.78 \pm 0.02$, in excellent agreement with $x = 0.8$ determined by Guérard *et al.* using chemical analysis.[4]

The presence of the hybridized graphitic states in C_8K which are zone folded to the Γ point by the $(2\times 2)R0^\circ$ K superlattice probably overextends the application of a simple two-carrier model to interpret a value for ω_p in this compound. Nevertheless, we proceed as follows to see what values of f_K are obtained. For the π band we use the numerical results for the optical mass obtained from Holzwarth[33] because the K point expansion of Blinowski *et al.*[32] is expected to break down for large f_C or large Fermi wave vector k_F. For the Γ point K($4s$) [or K($4s$)-π hybridized] electrons we use an isotropic mass m_K, and for charge neutrality we assume the relation $8f_C + f_K = 1$ (i.e., 1 e/K atom residing in either the π or K($4s$) band]. The plasma frequency ω_p is given [Eq. (2)] by $[(\omega_p^K)^2 + (\omega_p^\pi)^2]^{1/2}$, where ω_p^π and ω_p^K are the π and K($4s$) contributions. We find via numerical methods the self-consistent solutions for C_8K: (1) $f_K = 0.55$ for $m_K = 2m_e$, and (2) $f_K = 0.85$ for $m_K = m_e$. Thus we arrive at values for the K($4s$) band population in C_8K larger than the theoretical results by Ohno *et al.* ($f_K = 0.4$),[36] and much larger than that obtained by DiVincenzo and Rabii[37] ($f_K \sim 0$) (Table I). We note that the values for which we could obtain f_K by our simple two-band analysis would decrease further if increasingly larger values of m_K are used in the model. It is important to note that the values of f_K we have just obtained from the bare plasma frequency for C_8K are derived from a rigid-band model superimposing $2D$ π-electron bands and a $3D$ band for the K($4s$) electrons (m_{opt} for the Γ-point carrier pocket is the adjustable parameter). This model necessarily ignores altogether the potentially important effects of K($4s$)-π hybridization near the K and M points in the π^* band, which is a central issue in the debate between the more complete band models of C_8K.[36,37] Using their band-structure results ($f_K \sim 0$), DiVincenzo and Rabii[37] calculate a bare plasma frequency of 4.65 eV in good agreement with both our experimental value of $\omega_p = 4.5$ eV and the experimental value $\omega_p = 4.5$ eV obtained by Fischer *et al.*[27]

We next turn to the quantitative information which can be obtained from the interband absorption threshold. The threshold for interband absorption is identified with the rise in ϵ_2 with increasing ω after the fall due to the free-carrier contribution, and is evident Figs 3 and 4. The arrows in the figures indicate the midpoint of the respective interband threshold, which we refer to as E_T. If the interband threshold is due to transitions between carbon π (valence) and π^* (conduction) bands which have approximate mirror symmetry, then $E_T \sim 2E_F$. The bands near the K point in the model of Blinowski *et al.*[32] exhibit exact mirror symmetry (i.e., $E_T = 2E_F$), while the Holzwarth model[33] exhibits a slight asymmetry which introduces a correction δE at high charge transfer for donor-type GIC's (i.e., $E_T \sim E_F - \delta E$, where δE increases with increasing E_F ($\delta E \sim 0.1$ eV at $E_F \sim 1.4$ eV). Thus the π-π^* interband threshold represents another optical measure of E_F, independent of that obtained from the free-carrier plasma frequency. The π-π^* interband threshold has been shown by Shung[38] to be theoretically broadened about $\sim 2E_F$ due to electron scattering. Accordingly, we display in Table I the interband threshold energy E_T as the position of the midpoint of the initial rise in the interband contribution to ϵ_2. Good agreement is thereby obtained between E_F obtained from ω_p and that obtained from $E_T/2$ for $C_{24}K$, $C_4KH_{0.8}$ and $C_8KH_{0.8}$, indicating that in these compounds the interband thresholds are properly identified with π-π^* transitions. Values for f_C (number of electrons in π^* band per C atom) obtained from ω_p also appear in Table I. We note (Table I) that in the case of the stage-1 hydride, where E_F is large, the agreement between E_F (determined by ω_p) and $E_T/2$ is better within the Holzwarth model than in the Blinowski model. This is symptomatic of a breakdown of the K-point expansion approximation in the Blinowski model. We can compare our results for f_C and E_F in hydrides $C_4KH_{0.8}$ and $C_8KH_{0.8}$ to those obtained from Shubnikov–de Haas experiments by Enoki *et al.*[39] (Table I). Good agreement is obtained for the stage-2 hydride. However, agreement is not obtained for the stage-1 compound. The large disagreement in stage 1 may stem from the difficulty involved in observing the higher Shubnikov–de Haas frequencies.[43]

For the case of C_8K, we find $(E_T/2) = 1.6$ eV. Using the value $\delta E \sim 0.1$ yields a value for $E_F \sim 1.65$ eV, as compared to the value $E_F = 1.4$ eV obtained from both C_8K band-structure calculations.[36,37] Disagreement between π-electron-derived values of E_F and $E_T/2$ would be expected for C_8K on theoretical grounds because of the strong π-K($4s$) band hybridization near E_F and interband transitions near Γ to K($4s$)-derived states.[36,37] Our value of $E_T = 3.2$ eV compares reasonably well with the theoretical value of 2.9 eV calculated by both DiVincenzo and Rabii[37] and Ohno *et al.*[36] Fischer *et al.*[27] report an experimental value of 2.7 eV for the onset, rather than the midpoint, of the interband threshold. From their data[27] we estimate $E_T \sim 3.0$ eV in good agreement with our value.

IV. CONCLUSIONS

We find the graphite-KH_x optical data support the single-particle density of states shown in Fig. 5 in which the H($1s$) levels lie below E_F. The reflectance data were analyzed in terms of contributions from graphitic π elec-

trons and nearly free K(4s) electrons. The bare plasma frequencies we observe indicate the K(4s) band is empty (or nearly empty, $f_K \lesssim 0.03$) in the stage-1 and -2 hydrides, and empty in $C_{24}K$. We find ~ 0.20 electrons per K atom in the carbon π^* band(s) consistent with the stoichiometries $C_4KH_{0.8}$ (stage 1) and $C_8KH_{0.8}$ (stage 2) determined previously by chemical means.[4]

In the case of C_8K, the observed bare plasma frequency and position of the interband threshold are in good agreement with a previous experimental study[27] as well as band-structure calculations by DiVincenzo and Rabii.[37] The optical results for $C_{24}K$, $C_4KH_{0.8}$, and $C_8KH_{0.8}$ are found to be well described by a $2D$ graphitic π-electron model. A rigid, nonhybridized band model used to interpret the optical results in C_8K leads to values of $f_K < 0.5$ for values of the K(4s) electron optical mass $m_K > 2$, compared to theoretical estimates of $f_K = 0$ (DiVincenzo and Rabii[37]) and $f_K = 0.4$ (Ohno *et al.*[36]).

ACKNOWLEDGMENTS

We thank Dr. A. W. Moore of Union Carbide for his generous gift of the highly oriented pyrolytic graphite (HOPG) used in this study, Professor N. A. W. Holzwarth for original figures from her work in Ref. 33, and Professor J. P. Seleague for his guidance in preparing the KH powder for reaction. We are grateful to Professor H. Inokuchi and Dr. T. Enoki at the Institute for Molecular Science, Okazaki, for their efforts in organizing the recent topical conference on hydrogen in GIC's which we found very informative. The research was supported by the U.S. Department of Energy at the University of Kentucky (No. DE-EF05-84ER45151) and at Oak Ridge National Laboratory (No. DE-AC05-84OR2100), where one of us (P.C.E.) was on sabbatical leave during part of this research.

[1]D. Saehr and A. Hérold, Bull. Soc. Chim. Fr. 3130 (1965).
[2]M. Colin and A. Hérold, C, R, Acad. Sci C **269**, 1302 (1969).
[3]M. Colin and A. Hérold, Bull Soc. Chim Fr. 1982 (1971).
[4]D. Guérard, C. Takoudjou, and F. Rousseaux, Synth. Met. **7**, 43 (1983); D. Guérard, N. E. Elalem, and C. Takoudjou, *ibid.* **12**, 195 (1985).
[5]M. S. Dresselhaus and G. Dresselhaus, Adv. Phys. **30**, 139 (1981).
[6]S. A. Solin, Adv. Chem. Phys. **49**, 455 (1982).
[7]A. Hérold, D. Billoud, D. Guérard, P. Lagrange, and M. El Makrini, C. R. Acad. Sci. C **282**, 253 (1981); M. H. Yang, P. C. Eklund, and W. A. Kamitakahara, *Materials Research Society Proceedings of Symposium I: Intercalated Graphite, Boston, 1984,* edited by P. C. Eklund, M. S. Dresselhaus, and G. Dresselhaus, (Mat. Res. Soc., Pittsburg, 1984), p. 125.
[8]L. Salamanca-Riba, N. C. Yeh, T. Enoki, M. Endo, and M. S. Dresselhaus, in *Materials Research Society Proceedings of Symposium I: Intercalated Graphite,* Ref. 7, p. 249.
[9]G. Timp, T. C. Chieu, P. D. Dresselhaus, and G. Dresselhaus, Phys. Rev. B **29**, 6940 (1984).
[10]W. A. Kamitakahara, G. L. Doll, and P. C. Eklund, *Materials Research Society Proceedings of Symposium K: Intercalated Graphite, Boston, 1986;* edited by M. S. Dresselhaus, G. Dresselhaus, and S. A. Solin (Mat. Res. Soc., Pittsburgh, 1986), p. 69.
[11]K. Suzuki, I. Tsujikawa, M. Kobayaski, H. Inokuchi, Y. Oda, A. Sumiyama, H. Nagano, and Y. Kinishima, Synth. Met. **12**, 389 (1985).
[12]M. G. Alexander, D. P. Goshorn, D. Guérard, P. Lagrange, M. El Makrini, and D. G. Onn, Synth. Met. **2**, 203 (1980).
[13]N. C. Yeh, T. Enoki, L. Salamanca-Riba, and G. Dresselhaus, *Extended Abstracts of the 17th Binennial Conference on Carbon, Lexington, 1985,* edited by P. J. Reucroft and P. C. Eklund (University of Kentucky Press, Lexington, 1985), p. 194.
[14]N. C. Yeh, T. Enoki, L. McNeil, L. Salamanca-Riba, M. Endo, and G. Dresselhaus, in *Materials Research Society Proceedings of Symposium I: Intercalated Graphite,* Ref. 7, p. 246.
[15]T. Enoki, M. Sano, and H. Inokuchi, J. Chem. Phys. **78**, 2017 (1983).
[16]W. L. Jolly, *The Synthesis and Characterization of Inorganic Compounds* (Prentice-Hall, Englewood Cliffs, NJ, 1970), p. 136.
[17]P. C. Eklund, in *Intercalation in Layered Materials,* edited by M. S. Dresselhaus, (Plenum, New York, 1987), p. 323.
[18]D. M. Hoffman, R. E. Heinz, G. L. Doll, and P. C. Eklund, Phys. Rev. B **32**, 1278 (1985).
[19]P. C. Eklund, M. H. Yang, and G. L. Doll, in *Intercalation in Layered Materials,* Ref. 17, p. 257.
[20]M. S. Dresselhaus and G. Dresselhaus, in *Light Scattering in Solids III,* edited by M. Cardona and G. Güntherodt (Springer, Berlin, 1982), Chap. 2.
[21]P. C. Eklund and K. R. Subbaswamy, Phys. Rev. B **18**, 2020 (1978).
[22]R. J. Nemanich, S. A. Solin, D. Guérard, Phys. Rev. B **16**, 2965 (1977).
[23]P. C. Eklund, G. Dresselhaus, M. S. Dresselhaus, J. E. Fischer, Phys. Rev. B **21**, 4705 (1980).
[24]G. L. Doll and P. C. Eklund, in *Materials Research Society Proceedings of Symposium I: Intercalated Graphite,* Ref. 7, p. 110; G. L. Doll, P. C. Eklund, and J. E. Fischer (unpublished).
[25]L. G. Johnson and G. Dresselhaus, Phys. Rev. B **7**, 2275 (1973).
[26]E. A. Taft and H. R. Phillip, Phys. Rev. **138**, A 197 (1965).
[27]J. E. Fischer, J. M. Bloch, C. C. Shieh, M. E. Priel, and K. Jelly, Phys. Rev. B **31**, 4773 (1985).
[28]M. Zanini and J. E. Fischer, Mater. Sci. Eng. **31**, 169 (1977).
[29]L. A. Grunes and J. J. Ritsko, Phys. Rev. B **28**, 3439 (1983).
[30]M. E. Preil, L. A. Grunes, J. J. Ritsko, and J. E. Fischer, Phys. Rev. B **30**, 5852 (1984).
[31]L. A. Grunes, J. P. Gates, J. J. Ritsko, E. J. Mele, D. D. DiVincenzo, M. E. Preil, and J. E. Fischer, Phys. Rev. B **28**, 6681 (1983).
[32]J. Blinowski, N. H. Hau, C. Rigaux, J. P. Vieren, R. LeToullec, G. Furdin, A. Herold, and J. Melin, J. Phys. (Paris) **41**, 47 (1980).
[33]N. A. W. Holzwarth, Phys. Rev. B **21**, 3665 (1980).
[34]J. M. Zhang, D. M. Hoffman, and P. C. Eklund, Phys. Rev. B **34**, 4316 (1986).
[35]M. St. Jean, M. Menant, N. Hy Hau, C. Rigaux, and A. Metrot, Synth. Met. **8**, 189 (1983).

[36]T. Ohno, K. Nakao, and H. Kamimura, J. Phys. Soc. Jpn. **47**, 1125 (1979).
[37]D. D. DiVencenzo and S. Rabii, Phys. Rev. B **25**, 4110 (1982).
[38]K. W.-K. Shung Phys. Rev. B **34**, 1264 (1986).
[39]T. Enoki, N. C. Yeh, S. T. Chen, and M. S. Dresselhaus, Phys. Rev. B **33**, 1292 (1986).
[40]D. E. Nixon and G. S. Parry, and J. Phys. D **1**, 201 (1968).
[41]G. Dresselhaus, S. Y. Leung, M. Shayegan, and T. C. Chieu, Synth. Met. **2**, 321 (1980).
[42]S. Tanuma, H. Suematsu, K. Higuchi, R. Inada, and Y. Onuki, in *Proceedings of the Conference on the Application of High Magnetic Fields in Semiconductor Physics, New York, 1978,* edited by J. F. Ryan (Clarenden, Oxford, 1978), p. 85.
[43]M. S. Dresselhaus and N. C. Yeh (private communication).